ELSEVIER

Cement and Concrete Composites **20** (1998) 405–415
0958-9465/98/$ — see front matter

PII:S0958-9465(98)00011-0

A Filament Winding Technique for Manufacturing Cement Based Cross-ply Laminates

B. Mobasher* & A. Pivacek

Department of Civil and Environmental Engineering,Arizona State University, PO Box 875306, Tempe, AZ 85287-5306, USA

Abstract

A filament winding system was developed for manufacturing various types of fiber/cement composite materials. The system may be easily configured using the computer software to use continuous fiber composite laminates, cross-ply and angle ply laminates, pipes, and pultruded sections. The electrical and mechanical components of the system are discussed in detail. Cement based composite laminates are manufactured using continuous glass and polypropylene fibers. Tensile stress–strain response was measured using closed-loop strain controlled tests. Results indicate that tensile strength of composites can exceed 50 MPa using 5% alkali-resistant (AR) glass fibers. The ultimate strain capacity can also be increased by varying the stacking sequences. Ultimate strain capacities of the order of 2% were obtained. The experimental observations agree favorably with the theoretical predictions based on the ply discount method. © 1998 Elsevier Science Ltd. All rights reserved.

Keywords: fiber reinforced concrete, cememt composites, laminated composites, fibers, toughness, strength, microcracking, toughening, mechanical testing, manufacturing, glass fibers, polopropylene fibers.

INTRODUCTION

High Performance Fiber Reinforced Cement Composites (HPFRCC) materials have received significant attention in the past decade. Development of new materials is guided by an understanding of the interaction between the portland cement based matrix, fibers, and interface characteristics. The present work is aimed at development of processing techniques for manufacturing HPFRCC materials for severe loading conditions. These loading conditions may be defined through various tensile, impact, fatigue, and multiaxial loading criteria.

Cement based composites manufactured using the conventional processing techniques normally contain chopped random fibers. Theoretical approaches have demonstrated various mechanisms operative in increasing the strength, toughness, and fracture properties of the composites. The critical volume fraction of fibers necessary for distributed cracking has been studied by Li *et al.*,[1,2] and Naaman[3] using an energy balance criterion. Tjiptobroto and Hansen also used an energy balance approach to compute the strain at the end of multiple cracking region.[4] Yang *et al.* used a micromechanics approach to strengthening of the matrix phase and the critical volume fraction of fibers.[5,6] Mobasher and Li studied the strengthening and toughening mechanisms using a hybrid reinforcement system.[7] A major portion of the theoretical methods used concentrate on the toughening mechanisms in discrete fiber reinforced systems. However, both experimental and theoretical results show that increasing the aspect ratio of fibers significantly improves the mechanical performance of these composites. Despite such facts, new processing, manufacturing, and analysis techniques for continuous fiber cement based composite laminates have received little or no attention. Due to their sig-

*To whom correspondence should be addressed.

nificant strength and ductility improvement, these composites may prove to be the ideal choice for materials under severe loading conditions.

In the present work, composites are prepared with continuous fibers using the filament winding technique. The manufacturing system is computer controlled. It can be configured to make composite lamina, laminates, cross-ply and angle ply laminates, pipes, and pultruded sections. The effect of ply orientation and stacking sequence on the mechanical properties of these composites under tensile loading is studied.

THE FILAMENT WINDING SYSTEM

Computer aided manufacturing provides the agility, precision, and quality control needed to develop economic and versatile materials. The full potential of reinforcing fibers is utilized since the manufacturing technique is fully controlled and the composite laminates can be designed for the specific service loads they may encounter. The computer-controlled technique may significantly reduce the labor intensive manufacturing costs of construction products such as Glass Fiber Reinforced Concrete. It would certainly enhance the quality control aspects as compared to products of precast or cast-in-place concrete.

The mechanical components of the system consist of the feed, guide, and the take up (mold)sections. The electrical and electronics components consist of several servomotors, encoders, limit switches, and a computer. The computer uses object oriented programming languages to monitor a closed-loop system which controls at least two servomotors. Configuration of the servomotors determines the winding, pulling, and guidance of the composites, while the take up section controls the fiber (lamina) orientation. The components of the system are as follows:

Feed section

As shown in Fig. 1, the feed section consists of a single spool of fiber, a wetting tank, and an impregnation chamber. The glass or polypropylene fiber spool is mounted on a round steel bar that is connected to the setup table using frictionless bearings. The power to rotate the spool is supplied by an AC motor through a chain sprocket. A manually adjustable speed control may also be used to provide the torque to synchronize the rotation of the spool with the take-up section.

As the fiber roving unwinds from the spool, it passes over several round steel bars placed inside a water tank. The water dissolves some of the sizing and separates the fibers allowing infiltration of the paste. The roving is then partially drained off by passing over several bars above the water level. This process causes additional separation of the fibers.

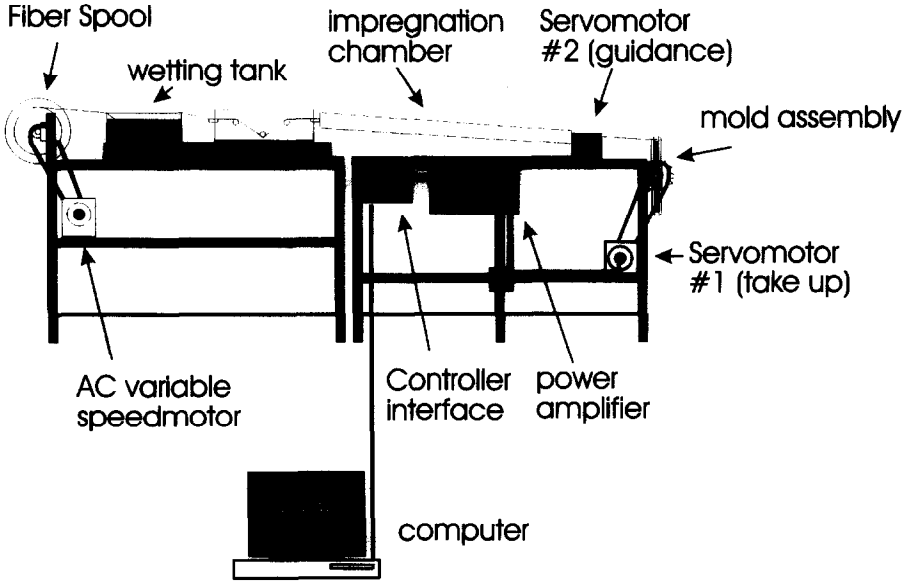

Fig. 1. Schematic side view of the filament winding setup.

The slurry infiltration chamber consisted of a tube 10 cm in diameter and 1.5 m long that was cut in half lengthwise. This tube was connected to the end of the tank and was filled with cement paste. A small mechanical vibrator was also used to aid the impregnation of the fiber along its travel path. Continuous vibration of the paste in the impregnation tube slowed down the partial setting along the fiber's path. The end of the slurry infiltration tube was placed on a sliding table platform that moved transverse to the fiber direction. Two cylindrical posts mounted on the platform align the fiber roving during its exit from the tube. The spacing between these two posts limited the amount of paste adhering to the fiber, thereby controlling the fiber volume fraction.

Guidance section

The linear positioning system as shown in Fig. 2 was used to guide the fiber roving onto the molds. The frictionless linear table slid on two solid shafts using four ball-bushing bearing pillow blocks. A precision drive screw with 10 threads per 25 mm moved the table on the guide arms for a total linear range of 45 cm. A direct drive servomotor connected to an 80:1 reduction gear, and a universal connection provided the necessary torque. An optical encoder was mounted at the end of the drive shaft to measure its rotation with an accuracy of 4000 counts per revolution. The displacement of the shaft was measured as a function of time and used to compute the velocity and acceleration. The programmed distance and speed of the servomotor determined the travel length and the amount of fiber placed on the mold. A limit switch was installed at each end of the linear position tables to disable the motor and terminate motion if the platform contacted the end assembly. Once a switch was activated, only motion in the opposite direction could be initiated. This backward motion of the table caused the switch to reset. This mechanism prevents accidental damage to the precision bolts.

Take up section

The specimens were made in the take-up section by the winding process. A typical mold consisted of two flat plexiglass plates

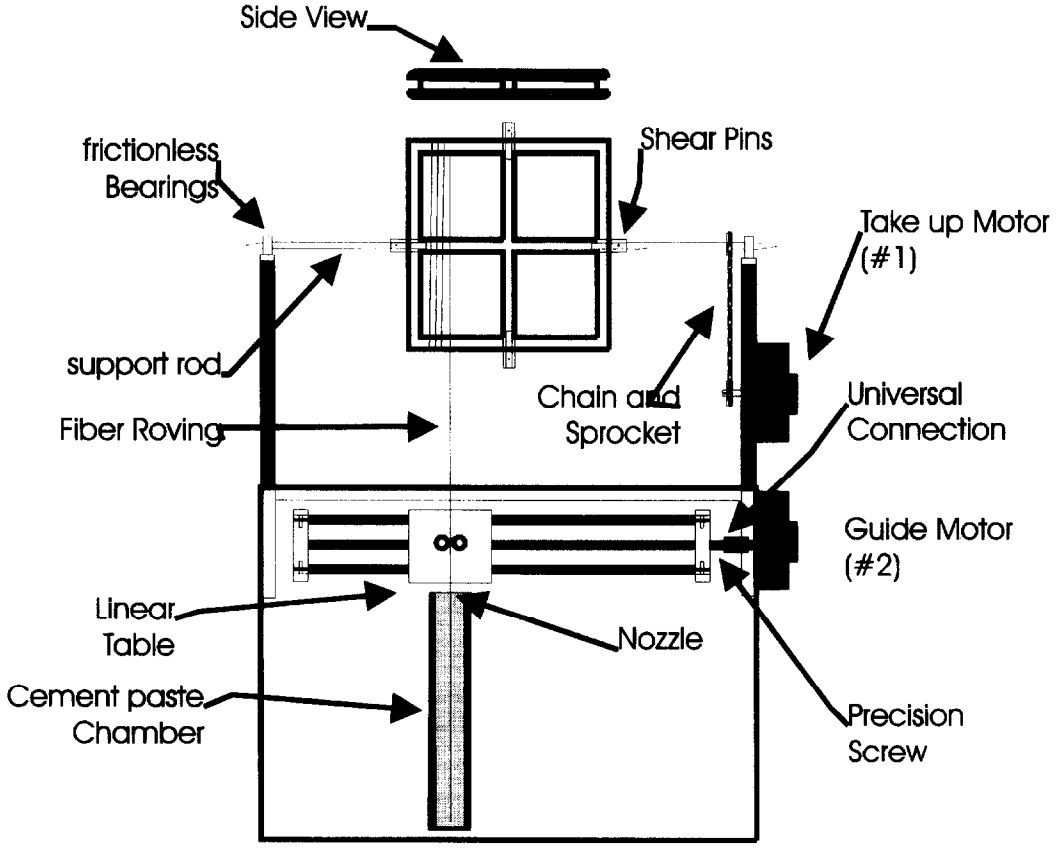

Fig. 2. Schematic drawing of the take-up section.

$50 \times 50 \times 1$ cm in dimensions separated by a spacer block $47.5 \times 47.5 \times 2.5$ cm in thickness. The four edges of the plates were machined to a fillet radius of 1 cm as shown in Fig. 2. The spacer block contained a series of guide slots with specific orientation. Orientation of the take-up mold with respect to the fiber winding could be easily changed during the winding process by switching the support rod from one guide slot to the other. The mold was connected to the drive rod using knuckled collars and shear pins. The drive rod was tapered down to a sharp point at both ends so that as the mold was rotated, the bar could pierce through the wound fibers. The steel bar was connected to the frame using frictionless bearings.

The mold assembly was chain driven by the second servomotor. Use of the chain drive facilitates mold rotation and alignment during the lay-up operation. A 1:1.5 sprocket ratio was used to transfer the torque from the servomotor to the rod.

ELECTRICAL SYSTEMS

The main components of the electrical system consisted of a 486 DX33 IBM compatible computer, a servo controller, servomotor amplifier, and a step-down transformer. The computer transferred the command motion signals to the controller, triggering the servomotor amplifier to provide the necessary electrical power to the motors. The step-down transformer supplied power to the amplifiers. The motion of the motor was measured and digitized by the optical encoders and the response was fed back to the computer for use in the closed-loop algorithms. To avoid water-associated hazards, waterproof cabling was used to protect the wiring and connections.

The software platform used for the computer control of the system was Labview®, an object oriented programming language. This software allows creation of modular programs to serve specific tasks referred to as "virtual instruments". These modular programs could be integrated into a simulated control panel.[8] The servo-controller was capable of handling the motions of up to four axes using the feedback from their respective encoder. Additional capabilities include torque limits, velocity limits, and end of travel on-off limit switches for clockwise and counter clockwise motion.

PROGRAM DEVELOPMENT

Several software modules are needed for any winding algorithm. A 'configuration module' was used to initialize the controller board, and set it up for specific winding requirements. A 'programming module' was then used for code development and automatic operation of the system, while a 'terminal module' allowed direct manual interaction with the linear motion system during the operational phase of specimen preparation.

Adjustment of servomotor motion parameters through closed-loop tuning allows optimal system performance and stability. The term 'closed-loop' indicates that the control of the system is based not only on the command signal but also on its response to the command. The feedback signal is measured from the encoders located on the back of both servomotors in terms of angular position with a resolution of 4000 counts per revolution. Using a gear ratio of 80:1, and a drive screw of 10 threads/25 mm results in a system resolution of 126000 counts/mm. The position signal is differentiated with respect to time to calculate the angular velocity and acceleration. These values are compared to the prescribed input values, and the difference between the measured input and the recorded output is referred to as the 'error'. The servo tuner changes the command signal using gain parameters that are dependent on Proportional, Integral, Velocity, and Feed-forward (PIVF) magnitude of the error. These tuning values are part of the system calibration during initial setup. After the first set up, tuning parameters for each motor are downloaded from the software. During the startup, the gain values for the motor as well as initial values for the motion parameters on each axis are downloaded and hard limit switches are enabled. Subsequently, the motors are energized and initialized to receive and execute input.

Specimen parameters include the sample width defined as d_2, layer orientation, and the ply thickness. Based on these parameters, the distances, velocities, and accelerations of each servomotor could be calculated and used as servomotor inputs. A deceleration rate equal to the acceleration value was used. The ply thickness and therefore the overall thickness depend on the velocity components of the two motors. For a constant take-up speed, V_1, the faster the guidance system V_2, the thinner the layer. To

establish a standard protocol, V_1 was set at 20 rpm, and V_2 was the independent parameter for controlling thickness. In order to ensure fibers laying down side by side (i.e. no gaps between the fiber roving on the mold) a maximum ratio of $V_2/V_1 = 0.5$ was used. The number of layers is determined by the number of passes by the guidance system and its speed. For example, a uniaxial piece of certain thickness can be made in one slow pass, or several passes. For a 0/90/90/0 sample, the guide speed can be reduced by 50% for the 90° pass to accomplish the desired thickness in a single pass. The distance of the take-up motor is determined by the ratio of the velocities multiplied by the guidance travel distance:

$$d_1 = d_2 \frac{V_1}{V_2} \tag{1}$$

The desired thickness of the sample determines the total number of encoder counts as d_2. The travel distance for the first servomotor (take up) is usually determined by the thickness of the layer desired. A ratio of d_1/d_2 between 2 and 3 was used. Higher values result in more revolutions over the same region, causing a thicker layer.

The algorithm for making uniaxial continuous fiber composites consists of several passes along the guide section and switching the sign of guide distance as the servomotor stops at the end of each pass. This is shown in Fig. 3. To make cross-ply laminates, motion was paused after a pass to remove the axis bar and rotate the mold by 90°. The motion was then resumed, rotating the mold for each ply.

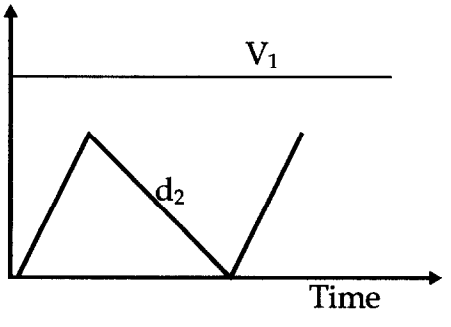

Fig. 3. Definition of distance and velocity parameters for making a four ply unidirectional lamina using three passes.

MATERIALS AND MIXTURES

The paste used in this study consisted of type I/II portland cement with a silica fume content of 10% by weight of cement. A water cementitious solids ratio of 0.35 was used. The silica fume was dispersed by premixing in a food processor. Mixing of the paste was done in a Hobart mixer. Properties of continuous AR Glass and Polypropylene (PP) fibers are shown in Table 1. The volume fraction of the fibers was measured using the cross sectional dimensions, the number of windings, and the cross sectional area of a single fiber strand. The same matrix formulation and a constant glass fiber volume fraction of 4.8% was used for all specimens studied in the present work.

After the windings were completed, the mold was removed from the bar and pressed at a constant pressure of 0.5 MPa under a hydraulic ram. The pressure was maintained for 3 h. The consolidation process removed excess water and resulted in reduced interlaminar porosity. For the cross-ply laminates, the average thickness of each ply was about 6 mm. The sample was covered in polyethylene sheets and placed in a curing room at 23°C, 95% RH for 24 h. After the first day of curing, the sample was sawed off from the Plexiglas mold using an angle grinder. Cutting was along the four edge slots of the mold. The sample was then placed in a water bath saturated with calcium hydroxide for 28 days.

The sample's rough edges were trimmed with a diamond blade saw, and several specimens 75 mm in width and 350 mm in length were cut from each panel. The surfaces were ground with a surface grinder to remove any excess. The samples were then shaped into dog bone specimens using a metal template. This was performed by a table router using a ceramic carbide bit. The approximate size of the cross section at reduced section was 50×20 mm material. The minimum width of the sample along the dog bone length was 50 mm. Perforated steel plates of $70 \times 75 \times 1.5$ mm dimensions were epoxied at the gripping sections of the specimen.

DISCUSSION OF RESULTS

Direct tension tests were performed on an MTS 810 closed-loop controlled servohydraulic

Table 1. Properties of the continuous fibers used in the present study

Fiber	*Source*	L_f (mm)	$d_f(\mu m)$	*Ultimate strength (MPa)*	*Elastic modulus (GPa)*	*Density (g/m^3)*
AR glass	Nippon Electric, Japan	Continuous	12	1725	70	2.70
PP	Krenit Fibers, Denmark	Continuous	35 × 250	340–500	8.5–12.5	0.91

material test system. The capacity of the loading frame was 220 KN (55 Kips). Hydraulic grips were used with the pressure in the grips maintained at between 5.0–7.5 MPa.

In the direct tensile tests, the elongation of the specimen across a 90 mm gage length was measured using two LVDTs of ±1.27 mm (±0.05 in) range. The LVDTs were mounted on both sides of the specimen, and their average response was used as the feedback control. The load and displacements were recorded by a data acquisition system with 12 bits resolution.

The tensile stress–strain response of the composites is shown in Fig. 4. Several features of both elastic and inelastic response are of interest. The initial elastic response follows the rule of mixtures quite closely. The average elastic moduli for composites are in the range of 21 ± 4 GPa which, based on the fiber volume fractions used, agrees favorably with the rules of mixtures. Results of all the tensile tests conducted are presented in Table 2. The numbers in parenthesis indicate the standard deviation of the sample population.

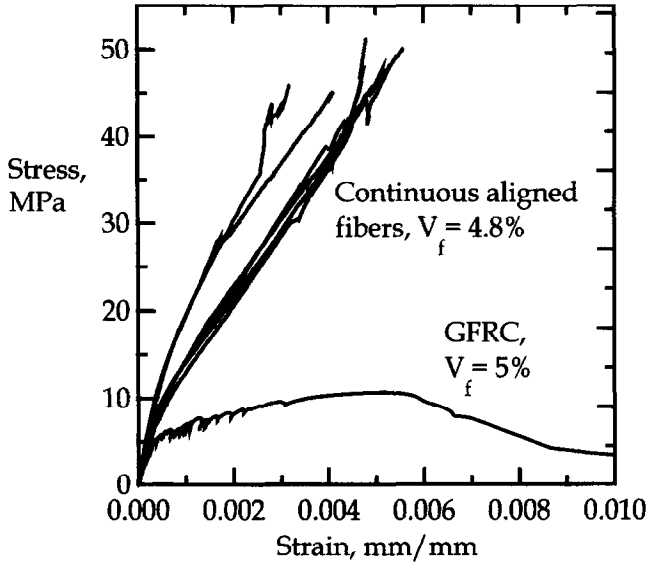

Fig. 4. Stress–strain response of unidirectional composites with AR glass fibers compared with GFRC.

The Bend-Over-Point (BOP) refers to the point where the ultimate strength of the brittle matrix phase in an FRC composite is reached. Although the BOP is quite evident in the composites with short fibers, in the present data, it is observed as a knee in the stress strain response. This is partly due to the significant stiffness of the fibers providing traction across the cracked matrix. This makes determination of the BOP difficult at best. Beyond the BOP point, the response remains linear up to the ultimate strength of the composites. The stiffness of the stress strain region between the BOP level and the ultimate strength was referred to as E_2. This parameter represents the equivalent elastic modulus of a composite containing matrix cracks. Due to the fracture of fibers at the point of ultimate strength, very little post peak ductility was observed. The failure was dominated by a complex interaction of fiber failure, matrix cracking, shear cracks in the composite, debonding and delamination, and crushing under the clamping pressure at the grips. The failure in the majority of the composites was associated with shear failure of composite at the interface between the fiber roving and the matrix. This mode of failure was also coupled with delamination between succes-

Table 2. Mechanical properties of glass fiber composite laminates

Lay up	*# of replicates*	*E* (GPa)	*Stress at BOP (MPa)*	*Strain at BOP*	*Ultimate strength (MPa)*	*Ultimate strain (mm/mm)*
0	9	23.6(4.4)	10.0(2.2)	4.11E-04(1.14E-04)	45.4(6.2)	7.6E-03(4.90E-03)
0/90/0	5	10.2(0.8)	5.2(1.0)	6.43E-042.30E-04	23.1(4.5)	1.44E-02(3.07E-03)
0/90/90/0	5	24.5(6.4)	11.8(3.8)	6.08E-4(3.95E-4)	38.3(9.2)	2.26E-2(1.29E-2)
90/0/90	4	11.6(7.6)	11.6(5.8)	1.27E-033.46E-04	31.5(7.0)	1.22E-02(2.67E-03)

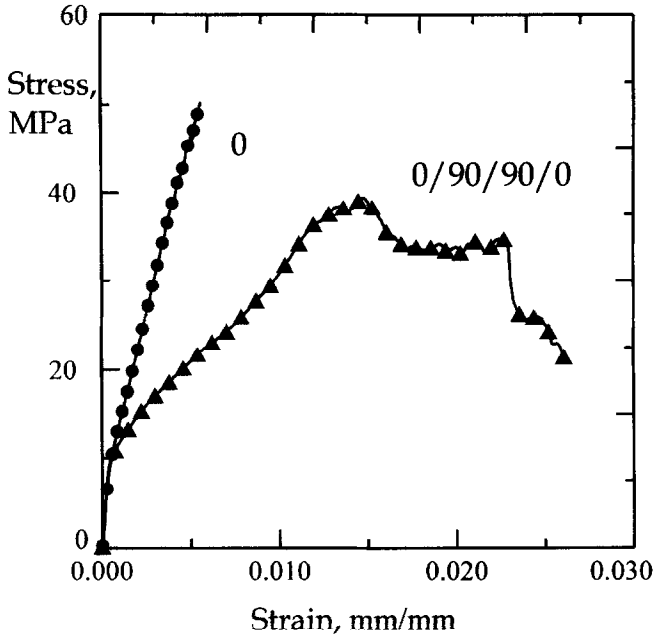

Fig. 5. Tensile response of composites with unidirectional fibers and a stacking sequence of 0/90/90/0.

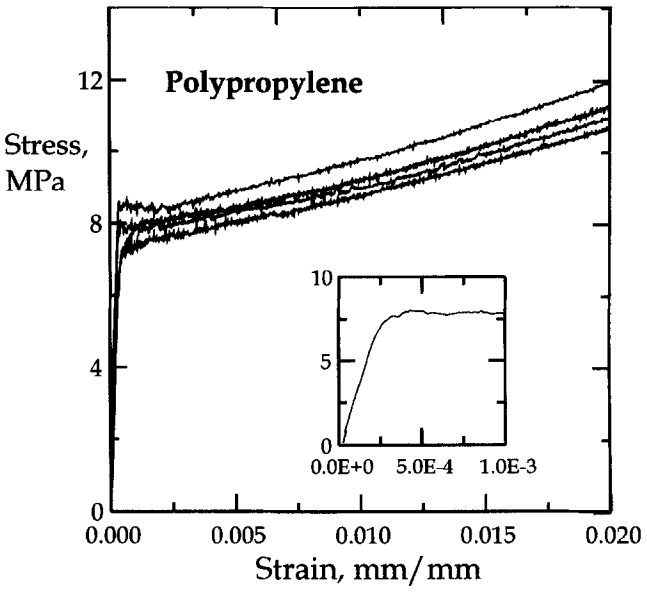

Fig. 7. Tensile response of composites with unidirectional polypropylene based fibers, $V_f = 7\%$. Inset shows the ascending part of the curve.

sive plies. In addition, significant cracking and crushing of the matrix material at the hydraulic grips was observed. The compression failure at the grips was furthermore associated with shear cracks along the load line. These shear cracks extended from the reduced section of the dog bone specimen to the grip.

The essential feature in the response of unidirectional 0° laminates was an ultimate strength of 50 MPa at an ultimate strain of 0.6%. Due to the various modes of failure involved, this strength level may not yet represent the strength of glass fibers. Results of Fig. 4 are also compared with the uniaxial tensile strength of commercially produced Glass fiber Reinforced Concrete (GFRC).[9] GFRC composites containing about 5% chopped AR glass fibers, are made by a spray-up process. It is noted that for the same comparable volume fraction of fibers, the strength of composites with continuous fibers is of the order of five times higher than the short, randomly distributed fiber composites.

Fig. 6. Microcracking in a three ply 90/0/90 composite (ply thickness≒6 mm).

The tensile response of a sample with 0/90/90/0-ply orientation is compared to a unidirectional sample in Fig. 5. Note that the strength of the composite is reduced to an approximate level of 40 MPa range, partly because the strength of the 90° plies in tension is closer to the tensile strength of the plain matrix. The ductility of the composite laminate however is significantly increased as compared to the unidirectional samples. Ultimate strain capacity is observed to be as high as 1.5% as compared to 0.6% for the unidirectional composites, an increase of 250%. The increase in ductility is attributed to two mechanisms of interlaminar cracking and parallel microcracking in the 90° plies. These two mechanisms result in a loss of stiffness in the composite, but an added degree of ductility is obtained. The increased strain capacity is clearly indicated as the specimen maintains tensile stresses of 35 MPa at strain levels as high as 2%. Fig. 6 represents the interlaminar cracking in a 90/0/90 composite. The extent of cracking in the 90° plies is indicative of the ability of the composite to distribute the microcracks throughout the matrix phase.

The tensile response of composites containing approx. 7% by volume of polypropylene

fibers is shown in Fig. 7. The inset in the figure shows the initial ascending portion of the curve. This region is characterized by a quasi-linear increase in stress up to approximate levels of 8 MPa. The bend over point is quite apparent in these composites. This level is a function of the fiber volume fraction, interface properties, and the matrix formulation. The present experimental results are comparable to the uniaxial tension results of composites pultruded manually by Stang and Krenchel.[10,11] Theoretical analysis for the prediction of BOP response has been provided using a fracture mechanics model.[12,13] The ultimate strain capacity of these composites is well beyond the 2% level shown in the figure. At this level of strain, significant distributed microcracking was observed in the specimens, and the load carrying capacity was primarily due to the straining of the fibers.

THEORETICAL EVALUATION

The experimental results of uniaxial tensions tests were compared using theoretical predictions of the classical laminate theory. A first order approximation based on the ply discount method was used.[14–16] In this method, an orthotropic model for the uniaxial response of a composite is used and the stiffness coefficients for the lamina are developed. The elastic responses of a single lamina and angle ply laminates are calculated next. An iterative procedure is followed next whereas the strain in the cross-ply lamina is incrementally increased and the stresses in each ply are computed. This stress level is compared to a stress based failure criterion, and once lamina failure is detected, the stiffness properties of that layer are updated. The procedure is continued for the entire strain domain.

A single ply is defined as a lamina and modeled as an orthotropic sheet in plane stress. The three principal material axis of the lamina are longitudinal and transverse to the fiber direction, and normal to the lamina surface are denoted as 1, 2, and 3 respectively. This is shown for the top ply of a 0/90/0 laminate in Fig. 8. It can be shown[17] that the constitutive relations for a general orthotropic material in the principal direction are:

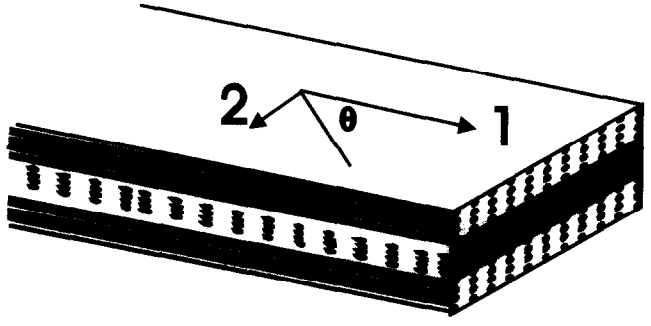

Fig. 8. Definition of the material axis for a 0/90/0 three ply composite laminate.

$$\varepsilon_j = S_{ij}\sigma_i; \quad \begin{bmatrix}\sigma_1\\ \sigma_2\\ \tau_{12}\end{bmatrix} = S_{ij}^{-1}\varepsilon_j = \begin{bmatrix}Q_{11} & Q_{12} & 0\\ Q_{21} & Q_{22} & 0\\ 0 & 0 & Q_{66}\end{bmatrix}\begin{bmatrix}\varepsilon_1\\ \varepsilon_2\\ \gamma_{12}\end{bmatrix} \tag{2}$$

where S is the compliance matrix and Q is the stiffness matrix, defined as:

$$S_{11} = \frac{1}{E_1}; S_{12} = -\frac{\nu_{12}}{E_1}; S_{22} = \frac{1}{E_2}; S_{66} = \frac{1}{G_{12}} \tag{3}$$

The stiffness of a lamina oriented at an angle θ, may be obtained by rotation of the axes by means of standard coordinate transformation procedures. By introducing the transformation matrix T, and R, the Reuter matrix as:

$$\begin{bmatrix}\sigma_1\\ \sigma_2\\ \tau_{12}\end{bmatrix} = T_{ij}\begin{bmatrix}\sigma_x\\ \sigma_y\\ \tau_{xy}\end{bmatrix} = \begin{bmatrix}\cos^2\theta & \sin^2\theta & 2\sin\theta\cos\theta\\ \sin^2\theta & \cos^2\theta & -\sin\theta\cos\theta\\ -\sin\theta\cos\theta & \sin\theta\cos\theta & \cos^2\theta-\sin^2\theta\end{bmatrix}\begin{bmatrix}\sigma_x\\ \sigma_y\\ \tau_{xy}\end{bmatrix}, R = \begin{bmatrix}1 & 0 & 0\\ 0 & 1 & 0\\ 0 & 0 & 2\end{bmatrix} \tag{4}$$

The stiffness for an arbitrary orientation angle is denoted as $\bar{Q}_{ij}$ and can be written as:

$$\bar{Q}_{ij} = T_{ij}RQ_{ij}RT_{ij}^{-1} \tag{5}$$

For a composite laminate consisting of several lamina each with an orientation of θ^m where m ranges from the first to the nth ply, the classical lamination theory results in derivation of lamina stiffness components as:

$$A_{ij} = \sum_{m=1}^{n} \bar{Q}_{ij}^m(h_m - h_{m-1}),\ B_{ij} = \frac{1}{2}\sum_{m=1}^{n} \bar{Q}_{ij}^m(h_m^2 - h_{m-1}^2),\ D_{ij} = \frac{1}{3}\sum_{m=1}^{n} \bar{Q}_{ij}^m(h_m^3 - h_{m-1}^3) \tag{6}$$

where A represents the extensional, D the bending, and B the coupling stiffness, and:

$$\begin{bmatrix}N\\ M\end{bmatrix} = \begin{bmatrix}A & B\\ B & D\end{bmatrix}\begin{bmatrix}\varepsilon^0\\ \kappa\end{bmatrix} \tag{7}$$

where M represents the moment per unit length, N the force per unit length of cross section, ε^0 and κ represent the mid-plane axial strain and the curvature of the section respectively. Using this approach, the stresses and strains in each lamina may be obtained by inverting the laminate constitutive relationship:

$$\begin{bmatrix}\varepsilon^0\\ \kappa\end{bmatrix} = \begin{bmatrix}A' & B'\\ B' & D'\end{bmatrix}\begin{bmatrix}N\\ M\end{bmatrix} \tag{8}$$

The form of submatrices A', B', and D' is discussed by Jones [17]. With knowledge of strain and curvatures, the stress in each lamina is computed. This procedure was used to analyze the failure of these composites using the first ply failure approach. An incremental procedure was used and the strains and forces were updated incrementally according to:

$$\begin{bmatrix}\Delta N\\ \Delta M\end{bmatrix} = \begin{bmatrix}\bar{A} & \bar{B}\\ \bar{B} & \bar{D}\end{bmatrix}\begin{bmatrix}\Delta\varepsilon^0\\ \Delta\kappa\end{bmatrix} \tag{9}$$

In a symmetric laminate there is no shear coupling effects and the submatrix $\bar{B}$ reduces to zero. For a state of uniaxial tension, eqn (9) reduces to:

$$[\Delta N] = [\bar{A}][\Delta\varepsilon^0] \tag{10}$$

where the $\bar{A}$ is modified at each increment to take into account the fact that some of the layers have fractured. After each failure, the incremental loads and strains are determined and the results are added to the loads and strains at the previous ply failure according to:

$$N_i^j = N_{i-1}^j + \Delta N_i^j \tag{11}$$

$$\varepsilon_i^j = \varepsilon_{i-1}^j + \Delta\varepsilon_i^j \tag{12}$$

where N is the nominal applied load. In the present calculations, the matrix and fiber elastic properties were used in the rule of mixtures to calculate the E_1. Calculation of the transverse modulus E_2 and ν_{12} was achieved using the Hal-

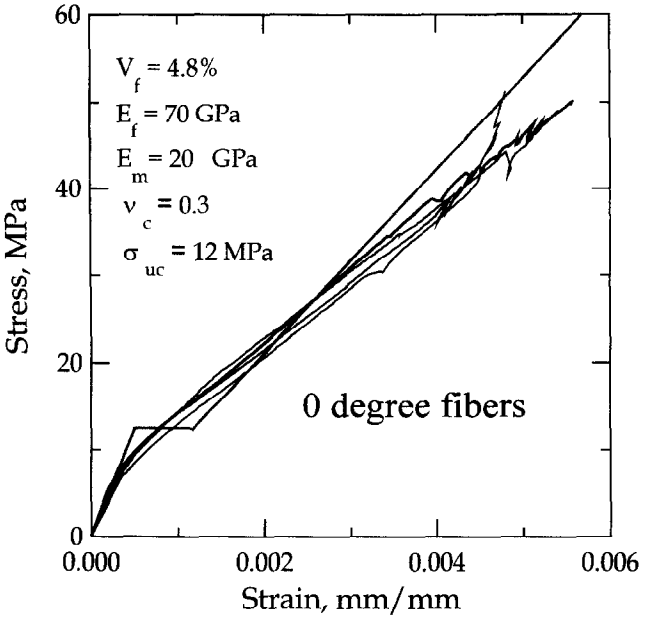

Fig. 9. Comparison of the theoretical and mechanical response of a three ply 0° laminate with a ply discount method.

pin-Tsai equations.[18] The strength of matrix in the presence of fibers depends on the mechanical properties, and volume fraction of the fibers, matrix, and the interface. Theoretical justification for evaluation of matrix strength has been provided in earlier work.[10] In the present case, strength of matrix equal to 12 MPa was used. Figure 9 represents the comparison of the ply discount method with the unidirectional fiber samples. Note that the experimental results exhibit a gradual transformation as the stiffness of the composite is degraded. In these composites only a single matrix crack was assumed. The stiffness of the composite across the crack was provided by the fibers. It was also assumed that no debonding or pullout processes are operative.

Figure 10 compares the prediction of ply discount method with two different composites, one with a 90/0/90 and the other with 0/90/90/0 orientation. In both cases it was assumed that at a stress level equivalent to 12 MPa, the 90° plies

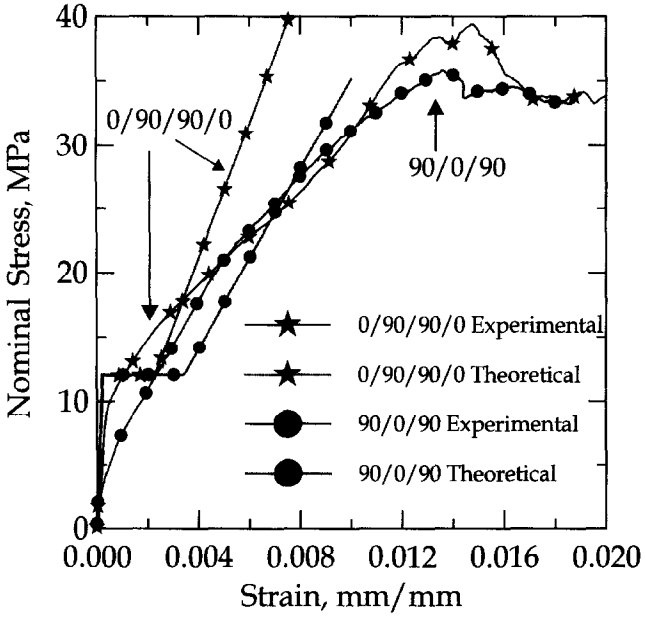

Fig. 10. Comparison of the mechanical response of a composite with a 90/0/90 and a composite with 0/90/90/0 with the ply discount method.

would fracture completely. The stiffness of the cracked plies was set equal to zero. The flat plateau in the composite with 90/0/90 orientation is longer since 2/3 of the specimen cross section is specified to crack. Once a ply is cracked, it is assumed that the load on that ply is transferred to the other plies as they carry the applied load. Note that both experimental data are quite close to each other suggesting that mechanisms such as ply delamination may be operative in both conditions. A stress analysis of the stacking sequence and determination of interlaminar shear stresses are required to further analyze the present data.

CONCLUSIONS

Cement based composite laminates were manufactured using a filament winding system. Mechanical response of composite laminates was measured using closed-loop uniaxial tensile tests. Results indicate that tensile strength of composites can reach in excess of 50 MPa. The weak phase in cross-ply composite laminates is the ply interface layer. Distributed cracking in the 90° plies results in toughening of the composites and the strain capacity is improved significantly. It was observed that cross-ply composite laminates with 5% AR glass fibers may carry in excess of 35 MPa at strain levels as high a 2%. Experimental results were compared to the ply discount method with favorable predictions.

ACKNOWLEDGEMENTS

Support of the National Science Foundation through the research initiation award # MSM-9211063, Program Director, Dr K. P. Chong is acknowledged. The authors thank Mr Henry Anderson of Engineering Computer Services and the entire staff of Engineering Laboratory Services at Arizona State University for their continuous support with instrumentation.

REFERENCES

1. Li, V. C. & Wu, H. C., Conditions for pseudo strain hardening in fiber reinforced brittle matrix composites. *Journal of Applied Mechanics Reviews*, **45**(8) (1992) 390–398.
2. Li, V. C. & Leung, C. K. Y., Theory of steady state and multiple cracking of random discontinuous fiber reinforced brittle matrix composites. *ASCE Journal of Engineering Mechanics*, **118**(11) (1992) 2246–2264.
3. Visalvanich, K. & Naaman, A. E., A fracture model for fiber reinforced concrete. *Journal of the American Concrete Institute*, **80** (2) (1983) 128–138.
4. Tjiptobroto, P. & Hansen, W., Tensile strain hardening and multiple cracking in high performance cement based composites. *ACI Materials Journal*, **90**(1) (1993) 0–00.
5. Yang, C. C., Mura, T. & Shah, S. P., Micromechanical theory and uniaxial tests of fiber reinforced cement composites. *Journal of Materials Research*, **6**(11) (1991) 2463–2473.
6. Li, S. H., Shah, S. P., Li, Z. & Mura, T., Micromechanical analysis of multiple fracture and evaluation of debonding behavior for fiber reinforced composites. International *Journal of Solids and Structures*, **30**(11) (1998), 1429–1459.
7. Mobasher, B. & Li, C. Y., Mechanical properties of hybrid cement based composites. *ACI Materials Journal*, **93**(3) (1996) 0–00.
8. *LabView Users Manual*. National Instruments, Austin, Texas, 1996.
9. Mobasher, B. & Shah, S. P., Test parameters in toughness evaluation of glass fiber reinforced concrete panels. *ACI Materials Journal*, **Sep/Oct** (1989) 448–458.
10. Krenchel, H. & Stang, H., Stable microcracking in cementitious materials. In *Brittle Matrix Composites 1*, eds A. M. Brandt, V. C. Li & I. H. Marshall. Woodhead Publishing Limited, 1994, pp. 20–33.
11. Mobasher, B., Stang, H. & Shah, S. P., Microcracking in fiber reinforced concrete. *Journal of Cement and Concrete Research*, **20** (1990) 665–676.
12. Mobasher, B. & Li, C. Y., Effect of interfacial properties on the crack propagation in cementitious composites. *Journal of Advanced Cement Based Materials*, **4**(3) (1996) 93–106.
13. Mobasher, B. & Li, C. Y., Modeling of stiffness degradation of the interfacial zone during fiber debonding. *Journal of Composites Engineering*, **5**(10/11) (1995) 1349–1365.
14. Talreja, R., Stiffness properties of composite laminates with matrix cracking and interior delamination. *Engineering Fracture Mechanics*, **25** (5/6) (1986) 751–762.
15. Allen, D. H., Harris, C. E. & Groves, S. E., A thermomechanical constitutive theory for elastic composites with distributed damage — I. theoretical development. *International Journal of Solids and Structures*, **23**(9) (1987) 1301–1318.
16. Allen, D. H., Harris, C. E. & Groves, S. E., A thermomechanical constitutive theory for elastic composites with distributed damage — ii. application to matrix cracking in laminated composites. *International Journal of Solids and Structures*, **23**(9) (1987) 1319–1338.
17. Jones, R. M., *Mechanics of Composites Materials*. McGraw Hill Book Co., New York, 1975.
18. Halpin, J. C. & Tsai, S. W., Environmental factors in composite materials design. Air Force Materials Research Laboratory, Technical Report, AFML-TR-67-423, 1967.